SHARING

SELF-ORGANIZED HETEROGENEOUS ADVANCED RADIO NETWORKS GENERATION

Deliverable D3.3

Advanced Transceivers and interference cancellation schemes at the receiver: Innovative Concepts and Performance Evaluation

Date of delivery	27/02/2015
Contractual date of delivery	27/02/2015
Project number	C2012/1-8
Editor(s)	Serdar Sezginer (SEQ)
Author(s)	Cécile Germond (TCS), Chien-Chun Cheng (SUP), Serdar Sezginer (SEQ)
Dissemination level	PU
Workpackage	3
Version	1.1
Total number of pages	26

Abstract:

This deliverable contains the evaluation of advanced transmitter and receiver techniques which are planned within Task3.2. Main focus is on novel schemes that can improve the system performance including low complexity interference cancellation algorithms targeting both uplink and downlink transmission and novel multiple-input multiple-output (MIMO) schemes, namely, enhanced spatial modulation.

Keywords: interference cancellation, multiple-input multiple-output (MIMO)

Document Revision History

Version	Date	Author	Summary of main changes
0.1	17/11/2014	All	Creation of thedocument including the Table of Contents (ToC)
0.2	08/12/2014	SEQ, SUP	SEQ-SUP contribution
0.3	15/12/2014	SEQ, SUP	Added missing references
0.4	22/12/2014	TCS, SEQ	TCS contribution (TCS) Introduction, Conclusion and Executive Summary parts (SEQ)
0.5	27/01/2015	SEQ, SUP	Update based on the reviewers comments on SEQ-SUP contributions.
0.6	28/01/2015	TCS	Update based on the reviewers comments on TCS contribution.
0.7	28/01/2015	SEQ	Accepted modifications, updated references and cleaned the comments.
0.8	24/02/2015	SEQ, TCS	Final version following the review comments from FT.
1.0	27/02/2015	SEQ	Final version

TABLE OF CONTENTS

LIST OF FIGURES

LIST OF TABLES

EXECUTIVE SUMMARY

This deliverable contains the evaluation of advanced transmitter and receiver techniques which are planned within Task3.2. Main focus is on novel schemes that can improve the system performance including low complexity interference cancellation algorithms targeting both uplink and downlink transmission and novel multiple-input multiple-output (MIMO) schemes, namely, enhanced spatial modulation.

Chapter 2 focuses on the optimization of the reception of useful signals and interference rejection techniques in LTE-A uplink. Multi antennas receivers are studied which are able to cope with internal (coming from other users in the LTE-A uplink) and external (coming from other than LTE-A uplink transmission) interferences in the presence of frequency selective fading channels. First, a summary of existing multiple antenna receivers in LTE-A uplink is provided. Then, an interference mitigation method is described and some preliminary results are presented. In order to propose a low complexity processing, we stick to a linear approach for the equalization and interference mitigation operations. Contrary to a classical minimum mean squared error (MMSE) approach, we do not assume a white Gaussian noise, hence we better take into account the properties of the noise and the interference when they are not white Gaussian.

In chapter 3, two new interference cancellation schemes are introduced, which provide further improvement of the UE reception performance compared to the interference rejection combining with diagonal loading (IRC-DL) scheme introduced in [1]. The idea is based on MMSE and successive interference cancelation (SIC) criteria, taking into account imperfect channel estimation and imperfect covariance estimation together with separately handling the interfering pilot and data signals. In addition, the optimal approach in the sense of the maximum likelihood (ML) detection is investigated as a benchmark for the performance evaluation of our proposed schemes. The numerical results show significant gain over IRC-DL proposed in [1] and the conventional schemes.

In chapter 4, the enhanced spatial modulation (ESM) technique, initially presented in [1], is extended, allowing multiple signal constellations to be used by different active antenna combinations. We show that spatial multiplexing (SMX) [5] and spatial modulation (SM) [6] offer significantly better performance compared to conventional MIMO schemes with equal spectral efficiency (i.e., same bits per channel use).

Finally, the main conclusions of this deliverable are presented together with the planned future contributions. For uplink interference cancellation, a particular focus will be put on the impact of channel estimation for the first processing, and on the number of available reference sequences for the second processing. On the downlink side, further investigation will be carried out for interference cancellation techniques focusing on the fundamental limits of the proposed one-dimensional model. Enhanced spatial modulation will also be explored further, on more complex constellations for higher throughput, on the basis of performance analysis and complexity evaluation.

1 INTRODUCTION

This deliverable contains the evaluation of advanced transmitter and receiver techniques which are planned within Task3.2. Main focus is on novel schemes that can improve the system performance including low complexity interference cancellation algorithms targeting both uplink and downlink transmission and novel multiple-input multiple-output (MIMO) schemes, namely, enhances spatial modulation.

A contribution is given on the interference mitigation in LTE-A focusing on uplink transmission. Single carrier waveform and frequency domain equalization are then considered. The environment is characterized by the presence of internal and external interferences and with a selective frequency fading. A first analysis of state-of-the art processing is performed. A processing is then defined, with a special requirement of low complexity, robustness, and good interference mitigation capabilities.

On the downlink side, two different topics have been tackled,namely, interference cancellation and enhanced spatial modulation (ESM).

For interference cancellation, two new schemes are introduced, which provide further improvement of the system performance compared to the model introduced in [1]. The idea is based on minimum mean squared error (MMSE) and successive interference cancelation (SIC) criteria, taking into account imperfect channel estimation and imperfect covariance estimation. In addition, the optimal approach in the sense of the maximum likelihood (ML) detection is investigated as a benchmark for the performance evaluation of our proposed schemes.

The ESM technique initially presented in [1]is extended allowing multiple signal constellations to be used by different active antenna combinations. Comparisons are provided with conventional MIMO schemes, such as SMX [5] and SM [6], at the same spectral efficiency.

2 ADVANCED INTERFERENCE MITIGATION IN THE UPLINK

2.1 Introduction

This chapter is focused on the optimization of the reception of useful signals and interference rejection techniques in LTE-A uplink. Single carrier waveform and frequency domain equalization are then considered. We look for multi antennas receivers able to cope with internal interferences (coming from other users in the LTE-A uplink) and externalinterferences (coming from other than LTE-A uplink transmissions) and when the fading of the propagation channel is frequency selective. The processing is defined, with a special requirement of low complexity and robustness. It will be followed by a performance study and practical implementation assessment in the following of the study.

We first give a summary of existing multiple antenna receivers in LTE-A uplink. As the exploitation of reference sequences is at the core of the studied processing, and of the proposed approach here, a description of the uplink LTE-A reference sequences is given. We then describe an interference mitigation method taking into account the presence of interference and provide some preliminary results.

In this chapter, we refer as SISO, SIMO and MIMO links for "Single Input Single Output", "Single Input Multiple Output", "Multiple Input Multiple Output", depending on the number of transmit antennas at the user equipment, and on the number of receive antennas at eNB.

2.2 State-of-the-art on interference mitigation in LTE uplink

In this paragraph, we make a quick overview of existing multiple antenna processing implemented in LTE-A uplink when several antennas can be exploited at reception.

Equalisation of SC-FDMA signals is usually linearly performed in the frequency domain, either with a Zero Forcing (ZF) - Frequency Domain Equalizer (FDE) or with a Minimum Mean Square Error (MMSE)-FDE. ZF completely cancels inter symbol interference (ISI) but leads to noise enhancement and thus performance degradation. MMSE takes into account the noise level in addition to ISI.

Let us consider a multi-user configuration where the Base Station(BS) is equipped with Nr antennas. There are K users. Two MIMO schemes are defined for SC-FDMA uplink transmission under 3GPP LTE, namely, multi-user MIMO and single-user MIMO. For a single user MIMO, the BS only schedules one single user into one RB. For a multi-user MIMO, multiple mobile stations (MSs) are allowed to transmit simultaneously on the same time/frequency slots, i.e. Resource Blocks (RB).

Let

- $[x_1^k, \ldots, x_M^k]$ be the DFT spread symbol of the kth user where M is the FFT size
- $\mathbf{h}_m^k$ be the component of the propagation channel between the kth user and the base station for the mth frequency sub carrier. $\mathbf{h}_m^k$ is a vector of dimension (N_r,1).
- n_m be the noise component at frequency m

The received signal vector on the mth frequency subcarrier is written as:

$$\mathbf{y}_m = \mathbf{H}_m \mathbf{x}_m + \mathbf{n}_m \quad (\text{Nr},1) \tag{1}$$

$$\mathbf{H}_m \triangleq [\mathbf{h}_m^1, \ldots, \mathbf{h}_m^K] \ (\text{Nr},K) \tag{2}$$

$$\mathbf{x}_m \triangleq [x_m^1, \ldots, x_m^K]^T \ (K,1) \tag{3}$$

The linear MMSE estimate of x_m^k is given by:

$$\hat{x}_m^k = \hat{\mathbf{w}}_m^H \mathbf{y}_m, \ m = 1, \ldots, M \tag{4}$$

where

$$\hat{\mathbf{w}}_m = \hat{\mathbf{R}}_{yy}^{-1}(m)\hat{\mathbf{r}}_{yrs}(m) \tag{5}$$

$\hat{\mathbf{R}}_{yy}(m)$ is the estimate of the covariance matrix of the received signal and $\hat{\mathbf{r}}_{yrs}$ is estimate of the correlation between the received signal and a reference sequence.

The linear MMSEreceiver minimizes the residual ISI energy and the noise.It is based on the hypothesis that the noise is spatially and temporally white and that there is no interference, which leads to the following expression:

$$\hat{\mathrm{x}}_{\mathrm{m}}^{\mathrm{k}} = \left(\mathbf{h}_{\mathrm{m}}^{\mathrm{k}}\right)^{\mathrm{H}} \left(\frac{1}{SNR}\mathbf{I}(N_r, N_r) + \mathbf{H}_{\mathrm{m}}\mathbf{H}_{\mathrm{m}}^{\mathrm{H}}\right)^{-1} \mathbf{y}_{\mathrm{m}},\ \mathrm{m} = 1, \ldots, \mathrm{M} \quad (6)$$

This processing is called MMSE-FREQ-MU in the sequel.

More complex schemes are analysed in the literature.

In [7], the authors propose a scheme based on a joint MMSE-FDE and SIC approach to perform the equalisation in a multi user context. Each user is allocated a specific set of frequency sub carriers, but transmits several spatially multiplexed streams thanks to the use of several antennas.The use of the SIC method, and the exploitation of Nr=Nt antennas at the eNB, allows to detect each data stream of each user.

The authors in [8]analyse 2 types of non linear receivers in the case of single antenna users scheduled on the same time/frequency slots. The Maximum Likelihood Detection (MLD) approach is based on a first FDE-MMSE filtering and then consists in a joint demodulation of the users, at a symbol by symbol rate, e.g. the detection of previous symbols is not taken into account for the detection of the current ones. The method compensates potential timing offsets between the users. A FDE-MMSE-SIC approach is also analysed. The non linear methods have better performance than the linear MMSE, but the latter is good enough provided there is enough diversity on the propagation channel.

In [9], the authors propose a FDE turbo equalizer of the LTE-A uplink. The method also allows to improve the estimation of the feedback parameters needed at the transmit side for closed loop spatial multiplexing schemes.

Turbo receivers for single user MIMO in LTE-A uplink are presented in [10]. A SIC and a Parallel Interference Cancellation(PIC) approaches are considered. At each iteration, the soft detection of each stream is cancelled from the received signal, either sequentially (SIC) or in parallel (PIC). The iterative process allows to improve the BER performance by several dBs. When the number of receive antennas increases compared to the number of multiplexed streams, the gain provided by the iterations gets smaller.

A SVD-based closed loop scheme is analysed for LTE-A uplink in [11]. The results show that is it preferable to improve the existing downlink codebooks for the uplink.

In a multi users context, [12] proposes a SIC like MMSE FDE equalizer which allows for a reduction of the level of inter symbol and inter antennas interferences.

[13]analyses a receiver method in the case where multiple users access the same time/frequency slots. They focus on the transmission of improper constellations, and hence propose an evolved MMSE-FDE with widely linear processing.

We can see that a first class of existing processing for the reception of LTE-A uplink signals leads to simple implementations (ZF, MMSE) but does not take account of the presence of interferers. Such processing are thus not reliable in an interference context. Another class of processing leads to more complex operations, such as MLD or non linear processing.

The objective here is to propose a low complexity processing having in mind a near-future implementation in radio products. This is why we are going to stick to a linear approach for the equalization and interference mitigation operations. The idea is now to take account of the properties of the possible interferers in order to better mitigate them. The solution is based on the use of LTE-A uplink sequence references.

2.3 Channel estimation – reference sequence

Most of the receiver processing need to estimate the propagation channel. This is the case for the linear MMSE receiver described above. Channel estimation is performed through the exploitation of reference sequences. In this study, we propose a processing also based on reference sequences. Hence, in this paragraph we give a brief description of the reference sequences used in the LTE uplink.

In the LTE uplink, each 1ms sub-frame is composed of 2 slots each composed of 7 symbols. Demodulation Reference Sequence (DMRS) are inserted in the 4^{th} and 11^{th} time symbols (when a normal length cyclic prefix is used). When a sub-frame is scheduled for channel sounding, the last symbol of the second slot of that subframe is reserved for a Sounding Reference Symbol (SRS).

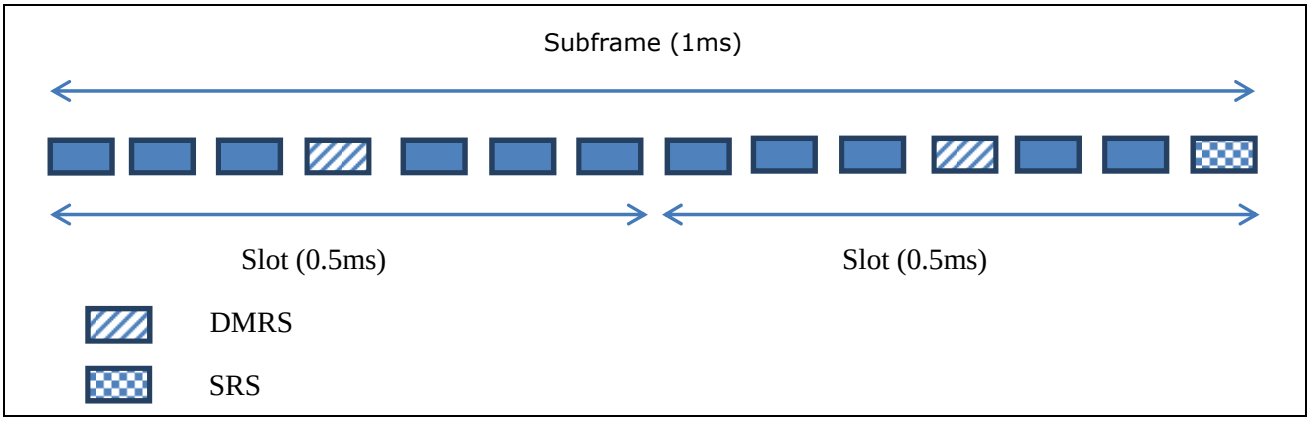

Figure 1 DMRS and SRS in LTE uplink

The time/frequency resource allocation is organised in RBs.

It is possible to multiplex on the same RBs several users (UEs) having each one single transmit antenna (MU-MIMO configuration). The estimation of the channel impulse responses (CIRs) is possible thanks to the use of cyclic shifted DMRS and/or SRS.

In LTE-A, each UE is assigned specific RBs in the uplink and can multiplex up to 4 data layers. Regarding channel estimation, the UEs can be separated through frequency division multiplexing. The CIRs of the layers of each UE can then be estimated thanks to the use of cyclic shifted DMRS.

A detailed description of the reference sequences can be found in [14].

2.4 Proposed method and preliminary results

In order to propose a low complexity processing, we stick to a linear approach for the equalization and interference mitigation operations.

The MMSE approach is selected and we take account of the possible presence of interferences. The receiver is then defined as:

$$\hat{x}_m^k = \hat{\mathbf{w}}_m^H \mathbf{y}_m, \ m = 1, \ldots, M \tag{7}$$

where

$$\hat{\mathbf{w}}_m = \hat{\mathbf{R}}_{yy}^{-1}(m)\hat{\mathbf{r}}_{yrs}(m) \tag{8}$$

Contrary to the MMSE-FREQ-MU approach described above, we do not assume a white Gaussian Noise, hence we better take account of the properties of the noise and interferences when they are not white Gaussian. The following estimates are computed thanks to the use of N_{rs} reference sequences.

$$\hat{\mathbf{R}}_{yy}(m) = \sum_{i=0}^{Nrs-1} y(m,i)y(m,i)^H \tag{9}$$

$$\hat{\mathbf{r}}_{yrs}(m) = \sum_{i=0}^{Nrs-1} y(m,i)rs(m,i)^* \tag{10}$$

The uplink LTE-A reference sequences presented above will be used.

This approach is called MMSE-FREQ-SU with colored noise. As interferences are part of the matrix $\hat{\mathbf{R}}_{yy}(m)$, the filtering with $\hat{\mathbf{R}}_{yy}^{-1}(m)$ allows for a better interference rejection than the classical approach of MMSE-FREQ-MU.

Both MMSE-FREQ-MU and MMSE-FREQ-SU "colored noise" processing are simulated and compared.

In this deliverable, we give preliminary results with the MMSE-FREQ-MU without and with interference, in order to show the degradation of the processing with interference.

Let us consider a configuration with 2 single antenna MSs scheduled on the same RBs. The eNBhas N_r antennas, with N_r=2 or 3. Rayleigh channels with one path are simulated. We assume a perfect knowledge of the propagation channels of both users.

The FFT size is set to 512 and the MSs use 96 sub carriers. 10^3 runs are performed.

Figure 2 presents the BER of the first MS when there is no interference. We can see the ability of processing several MSs scheduled on the same RBs. Performances improve with a larger number of receive antennas.

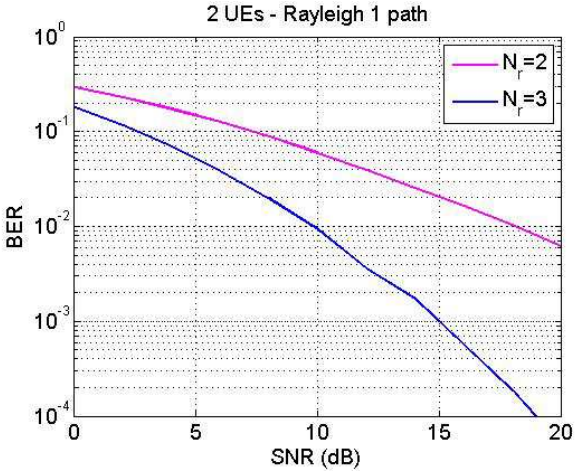

Figure 2 MMSE-FREQ-MU – no interference

Figure 3 presents the BER of the first MS with one interference and N_r=3. The interferer uses the same time/frequency resources than the MSs and propagates through the same kind of propagation channel, i.e. a Rayleigh channel with one path. The interferer/jammer to signal ratio (JSR) level is set to JSR=-∞, -15dB, -10dB, -5dB. We observe the degradation of performance when the JSR level increases.

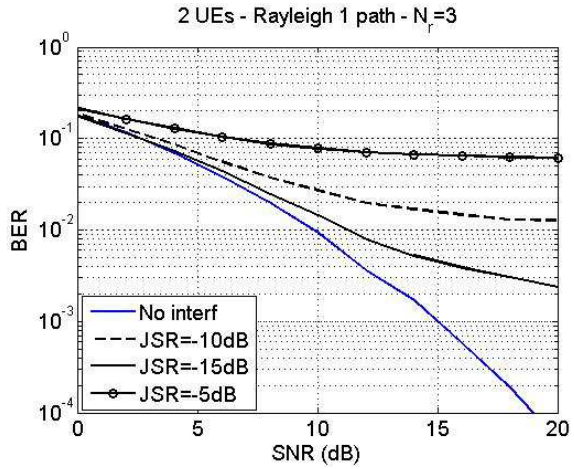

Figure 3 MMSE-FREQ-MU with interference

Results with the MMSE-FREQ-SU colored noise will be presented in the next deliverable.

2.5 Conclusion and next steps

In this chapter, we analyse receiver processing in the uplink of LTE-A which are able to equalize and mitigate internal and external interferences. We first recalled the most popular processing which is the linear MMSE processing performed in frequency domain and able to cope with multiple users. After a brief SOTA and description of the reference sequences used in LTE-A for channel estimation, we presented a processing which should better take into account the interferences and hence better mitigate them. First results have been presented with the SOTA processing referred to as MMSE-FREQ-MU processing.

Next work will carry on the comparison between the MMSE-FREQ-MU and the proposed MMSE with colored noise. A particular focus will be put on the impact of channel estimation for the first processing, and on the number of available reference sequences for the second processing. The goal is to assess the needed number of reference sequences for a good estimation of $\hat{\mathbf{R}}_{yy}(m)$and $\hat{\mathbf{r}}_{yrs}(m)$.

An extension of the processing with colored noise will be studied for a multi user case.

3 Interference Cancellation within Imperfect Channel Information in LTE DL Transmission

3.1 Introduction

In this contribution, we introduce two new interference cancellation schemes, which provide further improvement of the system performance compared to the model introduced in[1]. The idea is based on minimum mean squared error (MMSE) and successive interference cancelation (SIC) criteria, taking into account imperfect channel estimation and imperfect covariance estimation. In addition, the optimal approach in the sense of the maximum likelihood (ML) detection is investigated as a benchmark for the performance evaluation of our proposed schemes.

The main focus of these two schemes is to deal with the covariance matrices of the interfering pilot and the interfering data signal. In [1], we have found that the identically independent distribution (i.i.d.) does not hold for most of interference-limited scenarios in the currently deployed and specified communication systems [2]. This is because of the different format between the pilot and the data signals. In the sequel, we further derive two novel suppression schemes, namely LS-C, and LMMSE-C, based on the frame format of the 3GPP LTE downlink specifications [3]. The one-dimensional model introduced in [1] is used for our analysis and algorithm derivation. The numerical results show at least 5 dB SNR gain at $\mathbf{BER} = \mathbf{10^{-2}}$ over IRC-DL proposed in [1].

3.2 Proposed approaches

We consider a two-user Interference Channel (IC) for MIMO-OFDM systems. That means two eNodeBs use the same channel resource and are interfered each other because of serving their own users simultaneously. This model can be seen as four nodes as two transmitters and two receivers with intended links and interfering links between them. Assuming each node is equipped two antennas (numbers of transmit and receive antennas are $N_T = 2$, and $N_R = 2$), we start with a simplified model based on the LTE downlink received signal format as presented in [1].At the receiver side, since the desired signal and the interfering signaloccupy the same time and frequency resource, we can plot these resource blocks in two dimensions as shown in Figure 4 and present in one dimension as shown in Figure 5. In Figure 4, the frequency index is denoted by k as the y-axis and the time index is denoted by t for x-axis. Further, we point out the positions of the comb-type pilot symbols by using colored blocks with R_0 and R_1 in them. It can be observed from Figure 4and Figure 5 that the received signal is subject to different kinds of interference caused by the interfering pilot and data signals. In order to model this, we have to consider four different types of intervals depending on the pilot/data structure:

$$\mathbf{Y_p} = \mathbf{HX_p} + \boldsymbol{\alpha}\bar{\mathbf{H}}\bar{\mathbf{p}}\bar{\mathbf{X}}_{\mathbf{d1}} + \mathbf{Z_p} \in \mathcal{C}^{2\times 16} \quad (11)$$

$$\mathbf{Y_{d1}} = \mathbf{HpX_1} + \boldsymbol{\alpha}\bar{\mathbf{H}}\bar{\mathbf{p}}\bar{\mathbf{X}}_{\mathbf{d2}} + \mathbf{Z_{d1}} \in \mathcal{C}^{2\times(152-16)} \quad (12)$$

$$\mathbf{Y_{d2}} = \mathbf{HpX_2} + \boldsymbol{\alpha}\bar{\mathbf{H}}\bar{\mathbf{X}}_{\mathbf{p1}} + \mathbf{Z_{d2}} \in \mathcal{C}^{2\times 8} \quad (13)$$

$$\mathbf{Y_{d3}} = \mathbf{HpX_3} + \boldsymbol{\alpha}\bar{\mathbf{H}}\bar{\mathbf{X}}_{\mathbf{p2}} + \mathbf{Z_{d3}} \in \mathcal{C}^{2\times 8} \quad (14)$$

where $\mathbf{Y_p}, \mathbf{Y_{d1}}, \mathbf{Y_{d2}}, \mathbf{Y_{d3}}$ are the received signal matrices, $\mathbf{X_p}$ is the serving pilot matrix, $\mathbf{X_1}, \mathbf{X_2}, \mathbf{X_3}$ are the serving data matrices, $\bar{\mathbf{X}}_{\mathbf{d1}}, \bar{\mathbf{X}}_{\mathbf{d2}}$ are the interfering data matrices, $\bar{\mathbf{X}}_{\mathbf{p1}}$, $\bar{\mathbf{X}}_{\mathbf{p2}}$ are the interfering pilot matrices and $\mathbf{Z_p}, \mathbf{Z_{d1}}, \mathbf{Z_{d2}}, \mathbf{Z_{d3}}$ are AWGN matrices, α is a positive real number related to the signal-to-interference ratio (SIR), p, $\bar{\mathrm{p}}$ are the $N_T = 2$ dimensional precoding vectors with$N_T$denoting the number of transmit antennas, $\boldsymbol{H}$denotes the desired channel state information (CSI), and $\bar{\boldsymbol{H}}$denotes the interfering CSI.

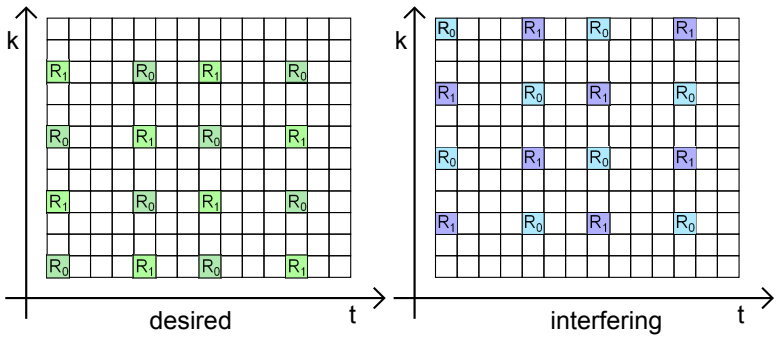

Figure 4 Mapping of the serving and interfering pilot symbols, where R_0 and R_1 indicate the pilot positions corresponding to the 1st and the 2nd transmit antenna ports, respectively

The conventional interference rejection combining (IRC) (which treats interference as a single Gaussian process and relies on linear MMSE (LMMSE) criterion) naturally leads to limited system performances. In [1], we show that the system performance can be highly raised by using our proposed scheme IRC-DL which considers interference as the multiple Gaussian processes. In this study, we propose new approaches based on two basic concepts: estimate the interfering pilot signal and compensate estimation errors.

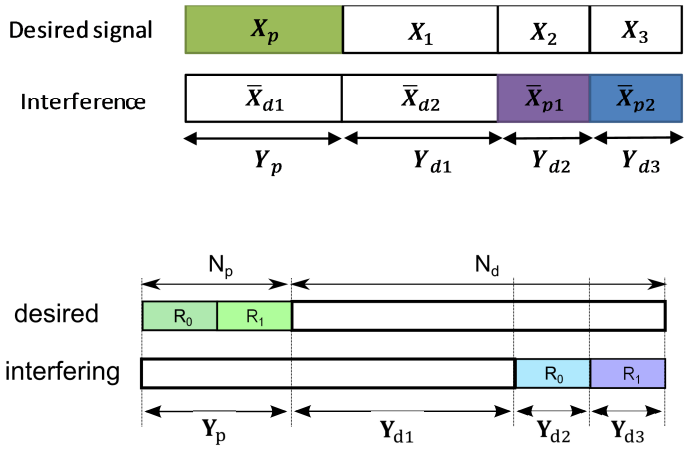

Figure 5 One-dimensional model arranging pilot and data symbols, where $N_p = 16$ denotes the length of the pilot signal and $N_d = 152$ is the length of the data signal

Least squares (LS) estimation with compensation (LS-C)

If the interfering pilot signal is perfectly known at the UEreceiver, we can apply the SIC to further improve the systemperformance. In this method, we regenerate the interferingpilot signal for decoding the data of interest. We rewrite thesystem model of the interfering pilot signal by combining thereceived signals of $\mathbf{Y}_{\mathrm{d2}}$ and $\mathbf{Y}_{\mathrm{d3}}$ given by (3) and (4) as

$$\mathbf{Y}'_{\mathrm{p}} = \mathbf{h}\mathbf{X}_{\mathrm{d1}} + \hat{\mathbf{h}}\bar{\mathbf{X}}_{\boldsymbol{p}} + \mathbf{Z}'_{\mathrm{p}} \in \mathcal{C}^{2\times \mathrm{N_p}}, \tag{15}$$

where the received matrix $\mathbf{Y}'_{\mathrm{p}} = [\mathbf{Y}_{\mathrm{d2}}, \mathbf{Y}_{\mathrm{d3}}]$ relates to the interfering pilot symbols, $\mathbf{X}_{\mathrm{d1}} = [\mathbf{X}_2, \mathbf{X}_3]$ denotes the serving data matrix,$\bar{\mathbf{X}}_{\boldsymbol{p}} = [\bar{\mathbf{X}}_{\boldsymbol{p1}}, \bar{\mathbf{X}}_{\boldsymbol{p2}}]$ denotes the interfering pilot matrix including the interfering symbols, and $\mathbf{Z}'_{\mathrm{p}} = [\mathbf{Z}_{\mathrm{d2}}, \mathbf{Z}_{\mathrm{d3}}]$ is the AWGN matrix. A simple LS channel estimator for both serving and interfering channels is thus given by

$$\hat{\mathbf{H}} = \frac{\mathbf{Y}_{\mathrm{p}}\mathbf{X}_{\mathrm{p}}^{\mathrm{H}}}{\mathrm{N_p}} = \mathbf{H} + \mathbf{E} \tag{16}$$

$$\hat{\mathbf{H}}_{\mathrm{b}} = \frac{\mathbf{Y}'_{\mathrm{p}}\bar{\mathbf{X}}_{\mathrm{p}}^{\mathrm{H}}}{\mathrm{N_p}} = \alpha\bar{\mathbf{H}} + \bar{\mathbf{E}}. \tag{17}$$

where$\hat{\mathbf{H}}$ is the estimate of the serving channel matrix, $\hat{\mathbf{H}}_{\mathrm{b}}$ isthe estimate of the interfering channel matrix, and the channelestimation errors are given by$\mathbf{E}$ and$\bar{\mathbf{E}}$.Once the interfering channel estimation is available, we regenerate the received pilot signal via the product of the channel estimate and the given pilot signal as $\hat{\mathbf{H}}_{\mathrm{b}}\bar{\mathbf{X}}_{\mathrm{p}}$. Therefore, the residual matrix of pilot cancellation is obtained as follows:

$$\hat{\mathbf{V}}_{\mathrm{b}} = \mathbf{Y}'_{\mathrm{p}} - \hat{\mathbf{H}}_{\mathrm{b}}\bar{\mathbf{X}}_{\mathrm{p}} = \mathbf{h}\mathbf{X}_{\mathrm{d1}} - \bar{\mathbf{E}}\bar{\mathbf{X}}_{\mathrm{p}} + \mathbf{Z}'_{\mathrm{p}} \in \mathcal{C}^{2\times \mathrm{N_p}}. \tag{18}$$

Considering the channel estimation errors on both the servingand interfering channels, we can derive the decoding metrics ofLS-C under the conditional LMMSE criterion as

$$\widehat{\mathbf{X}}_{\mathrm{d1,ls}} = \mathbf{w}_{\mathrm{ls}}^{\mathrm{H}}\widehat{\mathbf{V}}_{\mathrm{b}} \tag{19}$$

with

$$\mathbf{w}_{\mathrm{ls}}^{\mathrm{H}} = \arg\min \mathbb{E}\left[\left\|\mathbf{X}_{\mathrm{d1}} - \mathbf{w}^{\mathrm{H}}\widehat{\mathbf{V}}_{\mathrm{b}}\right\|^2 | \hat{\mathbf{h}}, \hat{\mathbf{h}}_{\mathrm{b}}\right] = \hat{\mathbf{h}}^{\mathrm{H}}\left(\frac{\mathrm{N_p^2}(\hat{\mathbf{h}}\hat{\mathbf{h}}^{\mathrm{H}})}{\mathrm{N_p^2}-1} + \frac{\mathrm{N_p^2}(\hat{\mathbf{h}}_{\mathrm{b}}\hat{\mathbf{h}}_{\mathrm{b}}^{\mathrm{H}})}{\mathrm{N_p^2}-1} + \mathrm{N}_0\mathbf{I}\right)^{-1}, \tag{20}$$

where$\hat{\mathbf{h}}_{\mathrm{b}} = \bar{\mathbf{p}}\widehat{\mathbf{H}}_{\mathrm{b}}$ is the equivalent interfering channel vector. This result is more complicatedthan the conventional solution that ignores channelestimation errors. The main difference can be seen in the equation (10) that the conditional expectation is given the estimated channel with channel estimation errors instead of the perfect channel knowledge, i.e.,$\mathbb{E}[\cdot|\hat{\boldsymbol{h}}, \hat{\mathbf{h}}_{\mathrm{b}}]$ instead of $\mathbb{E}[\cdot|\boldsymbol{h}, \mathbf{h}_{\mathrm{b}}]$. Indeed, the LS-C requires the precodingvector $\bar{\mathbf{p}}$to obtain the term of $\hat{\mathbf{h}}_{\mathbf{b}}$, which is not trivial to obtain inpractice. Therefore, an alternative way is derived by using thecovariance of the residual matrix. One can first noticethat the conditional covariance matrix of $\widehat{\mathbf{V}}$ is

$$\boldsymbol{\Sigma}_{\mathrm{v}} = \mathbb{E}\left[\widehat{\mathbf{V}}\widehat{\mathbf{V}}^{\mathrm{H}}|\hat{\mathbf{h}}, \hat{\mathbf{h}}_{\mathrm{b}}\right] = \frac{\mathrm{N_p^2}}{\mathrm{N_p^2}-1}\hat{\mathbf{h}}_{\mathrm{b}}\hat{\mathbf{h}}_{\mathrm{b}}^{\mathrm{H}} + \frac{\mathrm{N_p^2}}{\mathrm{N_p^2}-1}\hat{\mathbf{h}}\hat{\mathbf{h}}^{\mathrm{H}} + \mathrm{N}_0\mathbf{I}. \tag{21}$$

This covariance matrix is dominated by $\hat{\mathbf{h}}_{\mathrm{b}}\hat{\mathbf{h}}_{\mathrm{b}}^{\mathrm{H}}$, which is the term of interest. Substituting the covariance matrix Σ_{v} for the term of $\hat{\mathbf{h}}_{\mathrm{b}}\hat{\mathbf{h}}_{\mathrm{b}}^{\mathrm{H}}$, we have

$$\mathbf{w}_{\mathrm{ls}}^{\mathrm{H}} = \hat{\mathbf{h}}^{\mathrm{H}}\left(\hat{\mathbf{h}}\hat{\mathbf{h}}^{\mathrm{H}} + \frac{1}{\mathrm{N_p}}\boldsymbol{\Sigma}_{\mathrm{v}} + \frac{\mathrm{N_p}-1}{\mathrm{N_p}}\mathrm{N}_0\mathbf{I}\right)^{-1}, \tag{22}$$

which does not depend on the precoding vector $\bar{\mathbf{p}}$. Using thesample covariance estimation for the true covariance,$\widehat{\boldsymbol{\Sigma}}_{\mathrm{v}} = \frac{1}{\mathrm{N_p}}\widehat{\mathbf{V}}\widehat{\mathbf{V}}^{\mathrm{H}}$,the resulting output of LS-C becomes

$$\widehat{\mathbf{X}}_{\mathrm{d1,ls}} = \mathbf{w}_{\mathrm{ls}}^{\mathrm{H}}\widehat{\mathbf{V}}_{\mathrm{b}}\,, \tag{23}$$

where$\mathbf{w}_{\mathrm{ls}}^{\mathrm{H}}$ is obtained by using the sample covariance estimation $\widehat{\boldsymbol{\Sigma}}_{\mathrm{v}}$. Note that the LS-C is a mixed approach. We suppress the interfering data signal by its statistics and suppress the interfering pilot signal by regeneration and successive cancellation.

LMMSE with compensation (LMMSE-C)

It is possible to have the signal-to-interference ratio (SIR) information either from signaling or by estimation. In the presence of SIR, we can further improvethe channel estimation result by using the LMMSE channel estimator.The resulting output of the LMMSE estimator is obtained by

$$\mathrm{vec}\left(\widehat{\mathbf{H}}_{\mathrm{b,lm}}\right) = \overline{\mathbf{X}}_{\mathrm{pc}}^{\mathrm{H}}\left(\alpha^2\overline{\mathbf{X}}_{\mathrm{pc}}\overline{\mathbf{X}}_{\mathrm{pc}}^{\mathrm{H}} + \widehat{\boldsymbol{\Sigma}}_{\mathrm{vbc}}\right)^{-1}\mathbf{y}_{\mathrm{p}}',$$

where$\mathbf{y}_{\mathrm{p}}' = \mathrm{vec}(\mathbf{Y}_{\mathrm{p}}')$ is the vectorized form of the received matrix, $\widehat{\boldsymbol{\Sigma}}_{\mathrm{vbc}} = \mathbf{I}\otimes\left(\widehat{\mathbf{V}}_{\mathrm{b}}\widehat{\mathbf{V}}_{\mathrm{b}}^{\mathrm{H}}/\mathrm{N_p}\right)$is the residual matrix, and $\widehat{\mathbf{X}}_{\mathrm{pc}} = \overline{\mathbf{X}}_{\mathrm{p}}^{\mathrm{T}} \otimes \mathbf{I}$is the interfering pilot matrix. Replacing theLS channel estimates by the LMMSE channel estimates, we have the resulting output of LMMSE-C as

$$\widehat{\mathbf{X}}_{\mathrm{d1,lm}} = \mathbf{w}_{\mathrm{ls}}^{\mathrm{H}}\widehat{\mathbf{V}}_{\mathrm{b,lm}} \tag{24}$$

where$\widehat{\mathrm{V}}_{\mathrm{b,lm}} = \mathrm{Y}_{\mathrm{p}}' - \widehat{\mathrm{H}}_{\mathrm{b,lm}}\overline{\mathrm{X}}_{\mathrm{p}}$is the residual matrix of the LMMSE estimates. Note that the only difference between LS-C and LMMSE-C is the residual matrix $\widehat{\mathrm{V}}_{\mathrm{b,lm}}$. We only modify the residual matrix due to its substantial impacts on the system performance. This is verified in next sectionwith the numerical results.

3.3 Performance analysis

In this section, we provide the performance analysis of the proposed approaches. With these results we clarify the best achievable performance and the performance of the proposed approaches with respect to the optimal receiver.

Optimal receiver (OPT)

Let's first describe the optimal approach of the desired signal $x \in \boldsymbol{X}_1$ where the desired data signal suffers from the interfering data signal of the interferingeNB. The optimal receiver can be obtained by maximizing the posterior probability of the transmitted data signals given that the pilot symbols, the received vector $\mathbf{y} \in \mathbf{Y}_{\mathrm{d1}}$, precoding vectors, SNR and SIR are known.

$$\hat{\mathrm{x}} = \arg\max_{\mathrm{x}} \log \mathrm{P}\left(\mathrm{x}\middle|\mathbf{y}, \mathbf{Y}_{\mathrm{p}}, \mathbf{Y}'_{\mathrm{p}}, \mathbf{X}_{\mathrm{p}}, \bar{\mathbf{X}}_{\mathrm{p}}, \alpha, \mathbf{p}, \bar{\mathbf{p}}\right) = \arg\max_{\mathrm{x}} \sum_{\mathbf{X}_{\mathrm{d1}}, \bar{\mathbf{X}}_{\mathrm{d1}}, \bar{\mathrm{x}}} \frac{\exp(\mathbf{b}^{\mathbf{H}}\boldsymbol{\Sigma}^{-1}\mathbf{A}^{-1}\mathbf{b})}{\det(\mathbf{A})}, \tag{25}$$

where we apply the Gaussian integral[4] on the channel matrices and define the parameters as follows:

$$\mathcal{X} = \begin{bmatrix} \mathbf{X_p} & \mathbf{X_{d1}} & \mathbf{px} \\ \mathbf{p}\bar{\mathbf{X}}_{\mathbf{d1}} & \bar{\mathbf{p}}\bar{\mathbf{X}}_{\mathbf{p}} & \bar{\mathbf{p}}\bar{\mathbf{x}} \end{bmatrix} \tag{26}$$

$$\boldsymbol{\mathcal{Y}} = \left(\mathbf{Y_p}, \mathbf{Y'_p}, \mathbf{y}\right) \tag{27}$$

$$\mathbf{A} = \mathbf{I} + \boldsymbol{\Sigma}\left(\left(\frac{\mathcal{X}\mathcal{X}^{\mathbf{H}}}{\mathrm{N_0}}\right)^{\mathbf{T}} \otimes \mathbf{I}\right) \tag{28}$$

$$\mathbf{b} = \boldsymbol{\Sigma} \cdot \left(\frac{\mathcal{Y}\mathcal{X}^{\mathbf{H}}}{\mathrm{N_0}}\right) \tag{29}$$

$$\boldsymbol{\Sigma} = \begin{bmatrix} 1 & 0 \\ 0 & \alpha^2 \end{bmatrix} \otimes \mathbf{I} \tag{30}$$

The implementation of the OPT is not practical due to the summation of all possible candidates of the transmitted signals $\boldsymbol{X}_{d1}, \bar{\boldsymbol{X}}_{d1}$and $\bar{x}$. This formulation implies that we softly decode (compute all candidates) $\boldsymbol{X}_{d1}$ and $\bar{\boldsymbol{X}}_{d1}$ for better channel state information (CSI) estimates; and then softly decode $\bar{\mathrm{x}}$ to achieve maximum likelihood (ML) detection.

For comparison purposes, we show the performance bound by assuming that the interfering symbols $\bar{\boldsymbol{X}}_{d1}$ and the serving symbols $\mathrm{X_{d1}}$ can be decoded perfectly, i.e., both serving and interfering pilots are interference free. Thus, the resulting output can be rewritten as:

$$\hat{\mathrm{x}}_{\mathrm{opt}} = \arg\max_{\mathrm{x}} \log \sum_{\bar{\mathrm{x}}} \frac{\exp(\mathbf{b}^{\mathbf{H}}\boldsymbol{\Sigma}^{-1}\mathbf{A}^{-1}\mathbf{b})}{\det(\mathbf{A})} \tag{31}$$

This result can be used to evaluate the proposed algorithm. Note that the log-sum-exp operation can result in a computing problem, which can be solved by the log-sum-exp trick.

The OPT not only provides a performance boundary, but also enlightens our understanding of the two-user interference channel. We summarize our observations as follows:

- All interfering symbols $\bar{\mathbf{X}}_{\mathrm{d1}}$, $\bar{\mathbf{X}}_{\mathrm{d2}}$, and $\bar{\mathbf{X}}_{\mathrm{p}}$ should be decoded and subtracted in a decoding metric. Therefore, both the serving channel $\mathbf{H}$ and the interfering channel $\bar{\mathbf{H}}$ need to be estimated.
- Good quality of CSI is difficult to obtain because both the pilot symbols $\mathbf{X}_{\mathrm{p}}$ and $\bar{\mathbf{X}}_{\mathrm{p}}$interfere with the data symbols. On the other hand, these data symbols cannot be decoded and subtracted without reliable channel estimation. Therefore, the channel estimation errors on both channels $\mathbf{H}$, $\bar{\mathbf{H}}$ need to be compensated.

Moreover, it is worth noting that all information of interference is useful, but only some of it can be obtained easily. For example, the strength of interference (SIR) and the positions and the sequences of the interfering pilot symbols can be gathered on the UE side. However, perfect knowledge of the precoding vector and the modulation type of interference can only be obtained by decoding its control channels, which is not always feasible.

Numerical Results

In order to evaluate the proposed schemes, we consider a constant channel which is non-time-varying and frequency nonselective during $\mathrm{N_p} + \mathrm{N_d}$ intervals (within one RB). The data format follows the LTE frequency division duplexing (FDD) specifications given in Figure 4 and Figure 5 where we define $\mathrm{N_p} = 16$, and $\mathrm{N_d} = 152$. The data of interest $(\mathbf{X}_1, \mathbf{X}_2, \mathbf{X}_3)$ are modulated with Gray-coded $4-$QAM. The interfering data matrices $(\bar{\mathbf{X}}_{\mathrm{d1}}, \bar{\mathbf{X}}_{\mathrm{d2}})$ are modulated with Gray-coded $16-$QAM. In what follows, we

compare the performance of the conventional schemes: LMMSE (which treats interference as AWGN), IRC, and the proposed approaches: IRC-DL (see [1] for more details), LS-C, LMMSE-C, and OPT.

Figure 6 shows the BER performance of the presented schemes as a function of SNR with$\mathrm{SIR} = 0\,\mathrm{dB}$. These curves show the substantial improvements of the proposed schemes over the conventional solutions. The curve of IRC-DL shows the performance gain by interference suppression with proper grouping. Further improvement is achieved with cancelling the interference pilots as depicted with thecurves of LS-C and LMMSE-C. In this case, interfering pilot cancellation can get the largest performance gain. Moreover, the OPT shows the possible improvement if we can decode the interfering data symbols and further improve the channel estimation on both serving and interfering channels.

Figure 7 presents the BER performance of the presented schemes as a function of SIRs for $\mathrm{SNR} = 30\,\mathrm{dB}$. One can see that LS-C faces an error floorfor $\mathrm{SIR} \geq -10\,\mathrm{dB}$. This is because accurate CSI of interference is difficult to obtain under the weak interference assumption. This performance degradation can be highly reduced by using LMMSE-C.

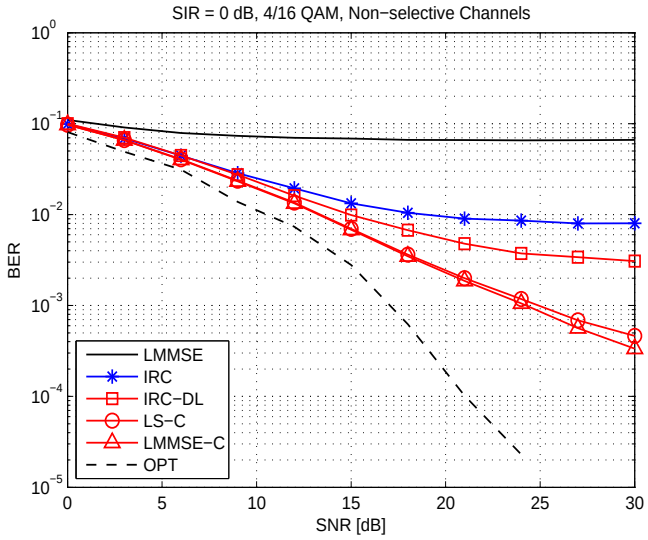

Figure 6 BER vs. SNR in the strong interference region, $SIR = 0dB$

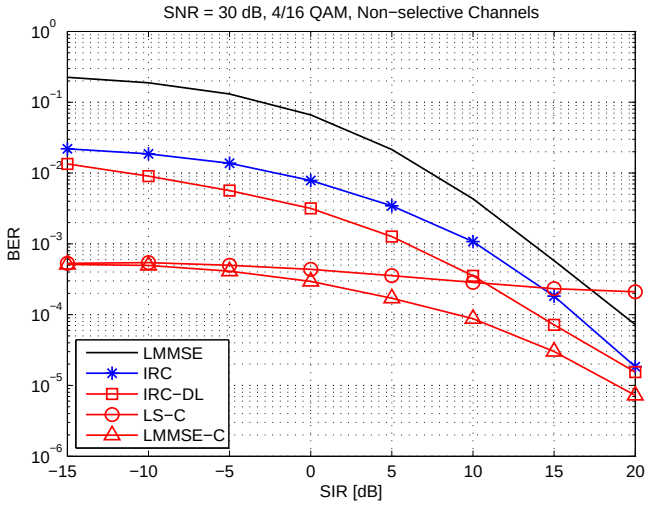

Figure 7 BER vs. SIR in the high SNR region, $SNR = 30\,dB$

3.4 Conclusions and next steps

This study considers interference suppression schemes for wireless communication systems. In such systems, the statistical property of interference impacts its suppression schemes. Therefore, given the pilot-data structure of interference, we derived novel schemes without the high cost of computation. Our results demonstrate that separately handling the interfering pilot and data signals allows substantial improvements. The simulations show that the largest performance gains are obtained when the interference is strong, at high SNR and without timing delay, because the interfering pilot signal can be cancelled accurately in this case. Consequently, in the presence of interference information advanced suppressions making use of this informationcan be considered in order to improve the system capacity.

Next, further investigation will be carried out focusing on the fundamental limits of the proposed one-dimensional model. We will investigate the different scenarios, including non-synchronized cases and triply selective channels where both the serving and the interfering channels are time variant, frequency selective and spatially correlated.

4 ENHANCED SPATIAL MODULATION SCHEMES

4.1 Introduction

Spatial Modulation (SM) has recently attracted significant attention. This technique exploits the multiple transmit antennas in a novel manner: It transmits information from a small subset of the transmit antennas in order to reduce the number of radio frequency (RF) chains. Specifically, some of the information bits are used to select the active transmit antennas, and the remaining information bits are mapped onto the constellation symbols transmitted from the selected active antennas.

In this study, we extend the contributionof enhanced spatial modulation (ESM) in [1] that allows multiple signal constellations to be used by different active antenna combinations. In order to achieve high spatial efficiency, the new technique, referred to as ESM-16QAM and ESM-64QAM, uses QAM as the primary modulation and reduced-size amplitude-phase modulation (APM) as the secondary modulation. Compared to conventional MIMO schemes, e.g., spatial multiplexing (SMX)[5]and spatial modulation (SM)[6], at the same spectral efficiency, ESM offers significantly better pair-wise error probability (PEP) performance. Moreover, the PEP performance analysis is also investigated, which shows that the design criterion of ESM can be based on the minimum Euclidean distance of the pairs of transmit symbols.

4.2 Proposed approaches

Following the same system model in [1], at the receiver the received signal can be written as:

$$\mathrm{y} = \mathrm{Hx} + \mathrm{n} \in \mathcal{C}^{\mathrm{N_R}}. \tag{32}$$

This model is the same as the conventional MIMO system model, however the main difference in SM systems is that only part of transmit (TX) antennas are activated. This property can be mathematically modeled by using zero elements in the transmitted vector, for example, $\boldsymbol{x} = [+1,0,0,0]$ denotes the symbol $+1$ is transmitted by using the first TX antenna, and $\boldsymbol{x} = [+1,-1,0,0]$ denotes two symbols transmitted simultaneously by using the first and the second TX antennas.When the channel state information is perfectly known at the receive side, the SM-type signal can be decoded by the ML decoder that estimates the transmitted symbol vector according to:

$$\hat{\mathrm{x}} = \arg\min_{\mathrm{x}\in\mathbb{x}} \|\mathrm{y} - \mathrm{Hx}\|^2, \tag{33}$$

where$\|\cdot\|$ denotes the vector norm, $\mathbb{x}$ denotes the constellation of the transmitted symbols, and the minimization is performed over all possible transmitted symbol vectors. Then we can have the union bound of the average BER as follows:

$$BER \leq \frac{1}{|\mathbb{x}|}\sum_{\boldsymbol{x}}\sum_{\boldsymbol{x}'\neq\boldsymbol{x}} b(\boldsymbol{x}\rightarrow\boldsymbol{x}')PEP(\boldsymbol{x}\rightarrow\boldsymbol{x}'),$$

where$|\cdot|$ is the cardinality that measures the number of elements of the set, and the function $b(\boldsymbol{x}\rightarrow\boldsymbol{x}')$ denotes the hamming distance between the two codewords (in terms of a bit level) respective to $\boldsymbol{x}$ and $\boldsymbol{x}'$, and $PEP(\boldsymbol{x}\rightarrow\boldsymbol{x}')$ is the pairwise error probability (PEP) as the probability that the ML decoder decodes a symbol vector x' instead of the transmitted symbol vector x. When the PEP is conditioned on CSI, it is defined as the conditional PEP,

$$P(\boldsymbol{x}\rightarrow\boldsymbol{x}'|\boldsymbol{H}) = Q\left(\sqrt{\frac{E_s}{2N_0}\|\boldsymbol{x}-\boldsymbol{x}'\|^2}\right),$$

where$Q(\cdot)$ denotes the Gaussian Q-function. The average PEP is obtained by averaging the conditional PEP over the probability distribution of the channel realizations. For Rayleigh fading channels, the average PEP is given by:

$$P(\boldsymbol{x}\rightarrow\boldsymbol{x}') = \frac{1}{\pi}\int_0^{\frac{\pi}{2}}\left(1+\frac{\rho}{4}\|\boldsymbol{x}-\boldsymbol{x}'\|^2\right)^{-N_R} d\beta \leq \left(1+\frac{E_s}{4N_0}\|\boldsymbol{x}-\boldsymbol{x}'\|^2\right)^{-N_R}$$

where$\rho = \frac{E_s}{N_0 \sin^2\beta}$ and the upper bound is obtainedby using the Chernoff bound. At high SNR, the error probabilityis dominated by the worst-case PEP, i.e., the system performance can be evaluated by the minimum vector normover all pairs of symbols:

$$L_{min} = \min_{\boldsymbol{x}\neq\boldsymbol{x}'} \|\boldsymbol{x}-\boldsymbol{x}'\|^2. \quad (34)$$

After averaging channel realizations, the PEP performance ofSM becomes independent of CSI. The main idea of ESM (see [1] for detailed explanation of ESM), whichis active Tx switching using information bits, turns into determining theindexes of the zero elements in the transmit symbol vector$\boldsymbol{x}$.Summarizing the above analysis, the goal of ESM is tohave a constellations set of the transmitted symbol vector,$\boldsymbol{x}$, for providing more combinations of the active Tx elementswhile maximizing the minimum Euclidean norm L_{min} in order toimprove the worst-cast PEP.

ESM with 16-QAM

For SM with 16QAM modulation and two Txantennas, 1 bit selects a transmit antenna, and 4 bitsselect a 16QAM symbol, and so, the conventional SM schemetransmits 5 bpcu. For ESM, we use the following antenna/constellationcombinations:

$$\mathbf{x}_{\mathrm{esm-16qam}} \in \left\{ \begin{bmatrix} \mathrm{x}_{16}^{(1)} \\ 0 \end{bmatrix}, \begin{bmatrix} 0 \\ \mathrm{x}_{16}^{(2)} \end{bmatrix}, \begin{bmatrix} \mathrm{x}_{\mathrm{q}_0}^{(1)} \\ \mathrm{x}_{\mathrm{q}_0}^{(2)} \end{bmatrix}, \begin{bmatrix} \mathrm{x}_{\mathrm{q}_1}^{(1)} \\ \mathrm{x}_{\mathrm{q}_1}^{(2)} \end{bmatrix} \right\}, \quad (35)$$

where$\mathrm{x}_{16}^{(\mathrm{k})}$ denotes a point of the 16QAM signal constellation, $\mathrm{x}_{\mathrm{q}_0}^{(\mathrm{k})} \in [1+\mathrm{i}, 1-\mathrm{i}, -1+\mathrm{i}, -1-\mathrm{i}]$, and $\mathrm{x}_{\mathrm{q}_1}^{(\mathrm{k})} \in [1, -1, \mathrm{i}, -\mathrm{i}]$. We refer to the signal constellations $\mathrm{x}_{\mathrm{q}_0}^{(\mathrm{k})}$ and $\mathrm{x}_{\mathrm{q}_1}^{(\mathrm{k})}$ as QPSK0 and QPSK1, respectively. These constellations are shown inFigure 8.Thecombinations used in ESM are those of Table II shown in §3.2of [1], when QPSK,BPSK0 and BPSK1 are replaced by 16QAM, QPSK0 andQPSK1,respectively. Note that the average power of theproposed constellation is larger than 16QAM, more specifically, $\mathrm{E_s} = 11$, and the points of the QPSK0 and QPSK1 constellations areplaced at the centers of the square grid formed by the primary16QAM constellation to maximize minimum Euclidean distance.Extension to the 4-Tx case follows the same process as inQPSK. Specifically, we just substitute in Table III given in §3.2 of[1] 16QAM, QPSK0,and QPSK1 for QPSK, BPSK0, and BPSK1, respectively.

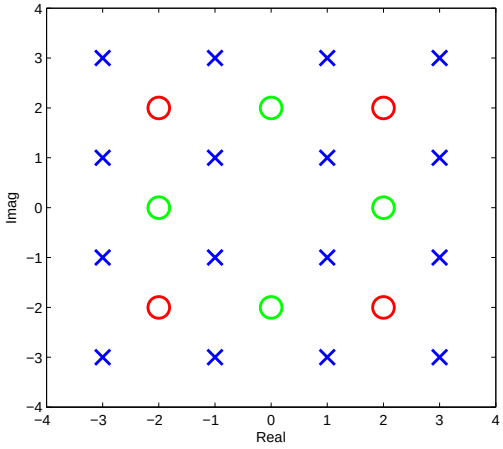

Figure 8 An illustration of the constellations used: The blue crosses represent 16QAM and the red (resp. green) circles represent the QPSK0 (resp. QPSK1) signal constellations

ESM with 64QAM

In order to achieve higher throughputs, we now describe ESM schemes using higher-level signal constellations. The design process is similar to that with the previous constellations, but here one has more degrees of freedom.The new ESM scheme is described using 64QAM as primary modulation and two TX antennas. ESM-64QAM is based on the following signal space:

$$\boldsymbol{x}_{esm-64qam} \in \left\{ \begin{bmatrix} \mathcal{C}_{64} \\ 0 \end{bmatrix}, \begin{bmatrix} 0 \\ \mathcal{C}_{64} \end{bmatrix}, \begin{bmatrix} \mathcal{A}_8^0 \\ \mathcal{A}_8^0 \end{bmatrix}, \begin{bmatrix} \mathcal{A}_8^1 \\ \mathcal{A}_8^1 \end{bmatrix} \right\},$$

where$\mathcal{C}_{64}$ denotes the 64QAM signal constellation used as primary modulation, and $\mathcal{A}_8^0$ and $\mathcal{A}_8^1$ represent two different secondary signal constellations of 8 points each. The secondary signal constellations are respectively given by $\mathcal{A}_8^0 = \{\pm 1 \pm i, \pm 4i, \pm 4\}$ and$\mathcal{A}_8^1 = \{\pm 1, \pm i, 4 + 2i, -4 - 2i, 2 - 4i, -2 + 4i\}$. These constellations are referred to as 8-Level Amplitude-Phase-Keying-Type 0 (8APK0) and 8-Level Amplitude-Phase-Keying-Type 1 (8APK1), respectively.The resulting ESM scheme, referred to 8-bpcu-2-Tx, transmits 8 bpcu. It can be verified that the average transmit signal power in this ESM scheme is $E_s = 33$. The constellations used are shown in Figure 9, where the signal points in 8APK0 and 8APK1 are placed close to the origin with the purpose of average power reduction. The combinations are the same as ESM-16QAM following the Table 2given in §3.2 of [1].

Extension to 4 TX antennas is straightforward. We simply replace QPSK, BPSK0, and BPSK1 in Table 3given in §3.2 of [1] by 64QAM, 8APK0, and 8APK1, respectively. The resulting scheme is referred to as 10-bpcu-4-Tx, because it transmits 10 bpcu.

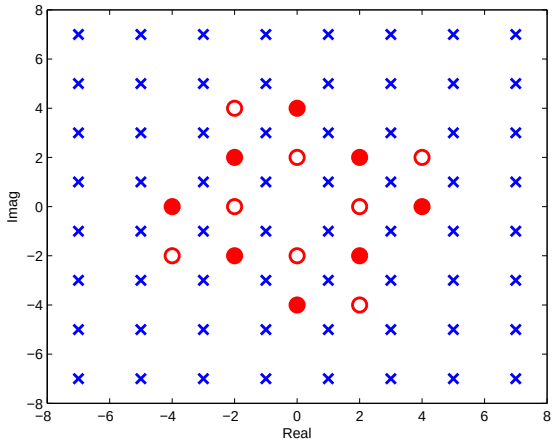

Figure 9 An illustration of the constellations used: The blue crosses represent 64QAM and the heavy/empty red circles represent the 8APK0/8APK1 signal constellations

4.3 Performance analysis

Worst case analysis

At high SNR, the PEP performance can be evaluated using$\mathrm{L} = \mathrm{L}_{\min}/\mathrm{E}_s$. Comparison of the minimum distance $\mathrm{L}_{\min}$ for different MIMO techniques is shown below in Table 1. For the 4-bpcu-2Txcolumn, it can be expected that SMX and ESM have the same PEP performance, and that both of them outperform SM. For 6-bpcu-2Tx, 6-bpcu-4Tx, and 8-bpcu-4Tx, ESM proves its benefits, providing a larger normalized $\mathrm{L}_{\min}$ than both SM and SMX.

Table 1 Minimum distance,$\mathrm{L}_{\min}$, for different MIMO techniques

	4-bpcu-2tx	6-bpcu-2tx/-4tx		8-bpcu-4tx
SM	0.5858	0.2	0.4	0.0952
SMX	1	0.2929		0.2
ESM	1	0.3636	1	0.3478

Note that withQPSK as primary modulation, bit labeling is important, because the minimum Euclidean distance in the signal space arises betweensymbol vectors that belong to different combinations. In this case, separately labeling the signal constellationsand the active antennas pattern is not optimum for ESM.However, this is an isolated case and the Euclidean distanceis preserved with higherlevel modulations, i.e., with 16QAM as primary modulationand QPSK0/QPSK1 as secondary modulations.

Numerical results

The numerical results were obtained using Rayleighfading MIMO channels with four receive antennas ($N_R = 4$).We comparedthePEP performances of different MIMO transmission schemes,based on the same number of transmitted bits per channel use.

Figure 10 and Figure 11 show the PEP performance corresponding tothe 6-bpcu-2-Tx and 8-bpcu-4-Tx cases, respectively. In bothcases, we can see that ESM provides substantial performanceimprovements over conventional SM and SMX. In particular,with the same number of Tx antennasas SMX, bettersystem performance can be achieved by ESM in the 6-bpcu-2-Tx case, as shown in Figure 10.

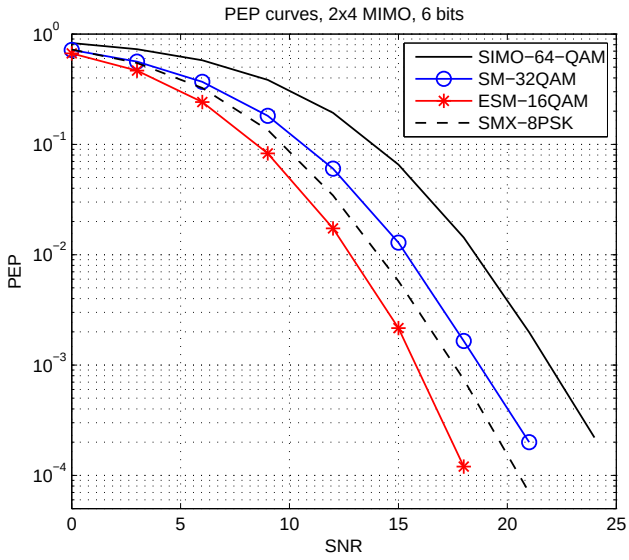

Figure 10 PEP curves for 6-bpcu-2-Tx

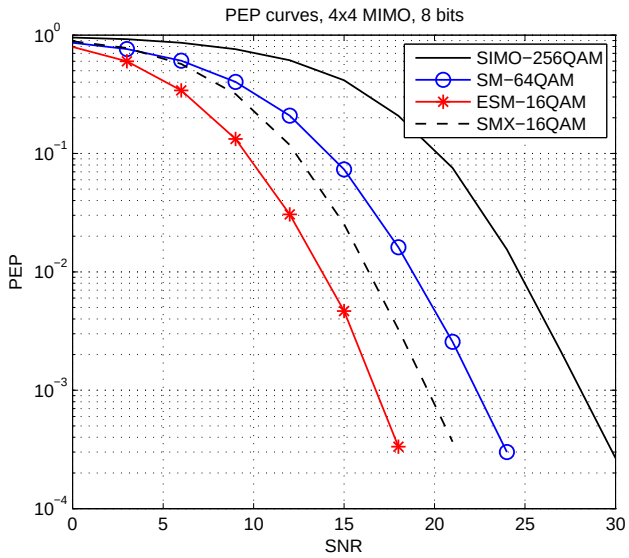

Figure 11 PEP curves for 8-bpcu-4-Tx

Next, in Figure 12, we show the PEP performance of 8-bpcu-2-Tx schemes in which ESM uses 64QAM as

primary modulation. The results indicate that ESM gains around 5 dB over SM, but loses close to 1 dB with respect to SMX at $PEP = 10^{-3}$.This performance loss is only shown in the part of 2TX cases and more performance gain can be achieved by ESM as the number of TX antennas increase.The average SNR loss of ESM is mainly due to the fact that combinations C1 - C2 use the 64QAM signal constellation while SMX uses 16QAM in that case.

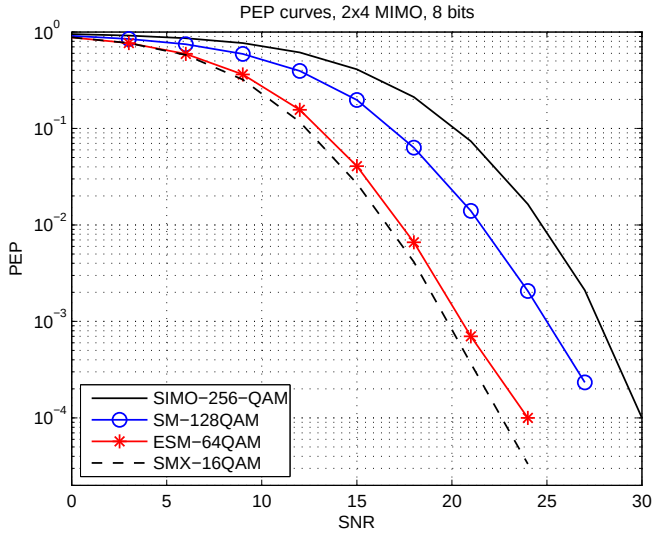

Figure 12 PEP curves for 8-bpcu-2-Tx

Figure 13 shows the PEP performance results of 10-bpcu-4-Tx in which ESM uses 64QAM as primary modulation. Here, ESM gains around 2 dB over SMX and more than 7 dB over conventional SM at $PEP = 10^{-3}$.The power penalty of conventional SM due to the use of dense constellations makes a serious impact in this case, and leads to a 5 dB SNR degradation.

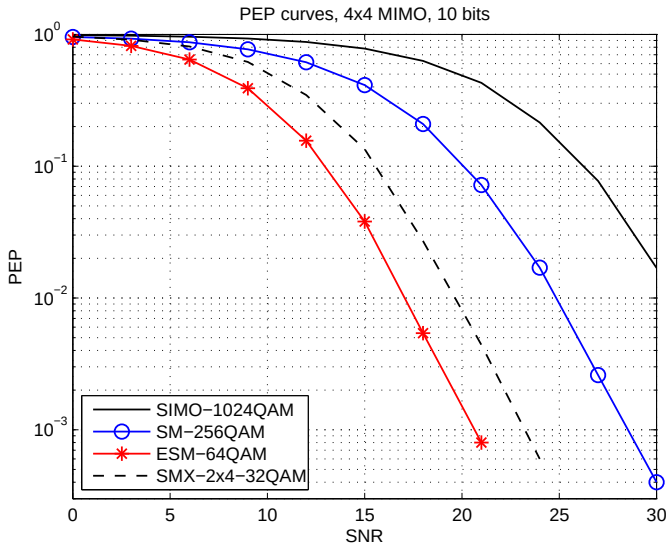

Figure 13 PEP curves for 10-bpcu-4-Tx

4.4 Conclusions and next steps

A new type of Spatial Modulation, referred to as ESM-16QAM and ESM-64QAM, has been presented by enabling one or two active Txantennas and using multiple signal constellations. On Rayleigh fadingchannels, we showed that the proposed technique outperformsconventional SM and SMX for the

same bpcu. More specifically, it can beseenthat with two TX antennas ESM potentially gains up to 6 dB over conventional SM and up to 2 dB over SMX. It was also found that with four TX antennas, ESM leads to higher gains: it gains up to 8 dB over SM and 2 dB over SMX.

The objective of the coming contributions will be the exploration of more complex constellation for higher throughput. The assessment of the proposed algorithms will be based on performance analysis and complexity evaluation.

5 CONCLUSIONS

This deliverable presented the advance transmitter and receiver techniques. Both uplink and downlink transmissions have been tackled.

On the uplink side, receiver processing in the context of LTE-A was analysed which is able to equalize and mitigate internal and external interferences. A processing has been presented taking into account the interferences and mitigating them in a better way.Next work will carry on the comparison between the proposed and the legacy methods. A particular focus will be put on the impact of channel estimation for the first processing, and on the number of available reference sequences for the second processing.

For the downlink transmission, two different aspects have been presented. First, interference suppression schemes for wireless communication systems have been studied. In such systems, the statistical property of interference impacts its suppression schemes. Using the pilot-data structure of interference, novel schemes have been derived without high computational cost. The results have demonstrated that separately handling the interfering pilot and data signals allows substantial improvements. The simulations show that the largest performance gains are obtained when the interference is strong, at high SNR and without timing delay, because the interfering pilot signal can be cancelled accurately in this case. Consequently, in the presence of interference information advanced suppressions making use of this information can be considered in order to improve the system capacity.Next, further investigation will be carried out focusing on the fundamental limits of the proposed one-dimensional model. Different scenarios will be investigated, including non-synchronized cases and triply selective channels where both the serving and the interfering channels are time variant, frequency selective and spatially correlated.

Second, new types of spatial modulation schemes, referred to as ESM-16QAM and ESM-64QAM, have been presented by enabling one or two active Txantennas and using multiple signal constellations. On Rayleigh fadingchannels, it has been showed that the proposed technique outperformsconventional SM and SMX for the same spectral efficiency. More specifically, it has been found that with two TX antennas ESM potentially gains up to 6 dB over conventional SM and up to 2 dB over SMX. It has been also found that with four TX antennas, ESM leads to higher gains: it gains up to 8 dB over SM and 2 dB over SMX.The objective of the coming contributions will be the exploration of more complex constellation for higher throughput. The assessment of the proposed algorithms will be based on performance analysis and complexity evaluation.

REFERENCES

[1] New opportunities, challenges and innovative concepts candidates for Multi-point transmission and reception, SHARING D3.1.

[2] A. Damnjanovic, J. Montojo, Y. Wei, T. Ji, T. Luo, M. Vajapeyam, T. Yoo, O. Song, and D. Malladi, "A survey on 3gpp heterogeneous networks," Wireless Communications, IEEE, vol. 18, no. 3, pp. 10–1, 2011.

[3] D. Bai, C. Park, J. Lee, H. Nguyen, J. Singh, A. Gupta, Z. Pi, T. Kim, C. Lim, M.-G. Kim, and I. Kang, "Lte-advanced modem design: challenges and perspectives," Communications Magazine, IEEE, vol. 50, no. 2, pp. 178–186, 2012.

[4] G. Taricco, "Optimum receiver design and performance analysis of arbitrarily correlated rician fading mimo channels with imperfect channel state information," Information Theory, IEEE Transactions on, vol. 56, no. 3, pp. 1114 –1134, march 2010.

[5] D. Tse and P. Viswanath, Fundamentals of wireless communication. Cambridge university press, 2005.

[6] R. Mesleh, H. Haas, S. Sinanovic, C. W. Ahn, and S. Yun, "Spatial modulation," IEEE Trans. Veh. Technol., vol. 57, no. 4, pp. 2228–2241, 2008.

[7] B. Sah& all, "A Frequency Domain Joint MMSE-SIC Equalizer for MIMO SC-FDMA LTE-A Uplink", IEEE 2014.

[8] M. Jiang & all, "Design of High Performance MIMO Receivers for LTE/LTE-A Uplink", IEEE 2010

[9] S. Ali Cheema & all, "Link Adaptation for LTE-A Systems Employing MMSE Turbo Equalization", WSA 2014.

[10]G.Berardinelli& all, "Turbo Receivers for Single User MIMO LTE-A Uplink", IEEE 2009

[11]G. Berardinelli& all, "SVD-based vs. Release 8 codebooks for Single User MIMO LTE-A Uplink", IEEE 2010.

[12]B.Yin& all, "Reconfigurable multi-standard uplink MIMO receiver with partial interference cancellation", IEEE ICC 2012.

[13]Z.Lin& all, "Analysis of Receiver Algorithms for LTE SC-FDMA Based Uplink MIMO Systems", IEEE trans. On Wireless Com., January 2010.

[14]X. Hou& all, "DMRS Design and Channel Estimation for LTE-Advanced MIMO Uplink", Vehicular Technology Conference (VTC Fall), 2009 IEEE 70th, 20-23Sept 2009.

GLOSSARY

ACRONYM	DEFINITION
3GPP	Third Generation Partnership Project
APM	Amplitude-Phase Modulation
AWGN	Additive White Gaussian Noise
BER	Bit Error Rate
BS	Base Station
CIR	Channel Impulse Response
CSI	Channel State Information
DMRS	Demodulation Reference Sequence
eNB	evolved Node B
ESM	Enhanced Spatial Modulation
FDD	Frequency Division Duplex
FDE	Frequency Domain Equalizer
IRC	Interference Rejection Combining
ISI	Inter Symbol Interference
JP	Joint Processing
JSR	Interferer/Jammer to Noise Ratio
JT	Joint Transmission
LMMSE	Linear Minimum Mean Square Error
LTE	Long Term Evolution
LTE-A	Long Term Evolution - Advanced
MIMO	Multiple Input Multiple Output
ML	Maximum Likelihood
MLD	Maximum Likelihood Detection
MMSE	Minimum Mean Square Error
MS	Mobile Station
MU-MIMO	Multiple User MIMO
PEP	Pairwise Error Probability
PIC	Parallel Interference Cancellation
SIC	Successive Interference Cancellation
SIMO	Single Input Multiple Output
SIR	Signal to Interference Ratio
SISO	Single Input Single Output
SM	Spatial Modulation

SMX	Spatial Multiplexing
SNR	Signal to Noise Ratio
SRS	Sounding Reference Symbol
RB	Resource Block
UE	User Equipment
ZF	Zero Forcing